

Comparative Analysis of UAV Path Planning Algorithms for Efficient Navigation in Urban 3D Environments

1st Hichem Cheriet

dept. of Computer Science

Université d'USTO Mohamed Boudiaf

Oran, Algeria

hichem.cheriet@univ-usto.dz

2nd Khellat Kihel Badra

dept. of Economics

Oran2 Mohamed BenAhmed University

Oran, Algeria

khellat_badra@yahoo.fr

3rd Chouraqui Samira

dept. of Computer Science

Université d'USTO Mohamed Boudiaf

Oran, Algeria

samirachouraqui178@gmail.com

Abstract—The most crucial challenges for UAVs are planning paths and avoiding obstacles in their way. In recent years, a wide variety of path-planning algorithms have been developed. These algorithms have successfully solved path-planning problems; however, they suffer from multiple challenges and limitations. To test the effectiveness and efficiency of three widely used algorithms, namely A*, RRT*, and Particle Swarm Optimization (PSO), this paper conducts extensive experiments in 3D urban city environments cluttered with obstacles. Three experiments were designed with two scenarios each to test the aforementioned algorithms. These experiments consider different city map sizes, different altitudes, and varying obstacle densities and sizes in the environment. According to the experimental results, the A* algorithm outperforms the others in both computation efficiency and path quality. PSO is especially suitable for tight turns and dense environments, and RRT* offers a balance and works well across all experiments due to its randomized approach to finding solutions.

Index Terms—Unmanned Aerial Vehicle, Path Planning, A* Algorithm, Comparative Analysis, RRT*, PSO

I. INTRODUCTION

Unmanned aerial vehicles (UAVs) with different shapes and types are widely utilized in many fields, such as military [2], photography, search and rescue [3], and agriculture [1]. The path-finding problem has been a key area of research these years for effectively navigating terrains, successfully completing missions, and arriving at target positions. Path planning, in general, can be separated into two principal approaches. The first approach is used when the environment is already known, and the threats maintain their position without movement, such as buildings, bridges, and traffic lights. This is called static path planning, referring to the static environment. Path planning for this type is calculated before the mission starts. The second type is called dynamic path planning, referring to the dynamic environment where obstacles change their positions, such as vehicles, birds, humans, etc. Dynamic path planning requires an online path calculator in the UAV to adapt to any environmental changes effectively. The choice between these two approaches depends on the mission requirement.

Path planning algorithms can be categorized into four main approaches. Firstly, graph-based search algorithms treat the

environment as a graph. In this approach, nodes represent specific locations or states, and edges represent possible transitions or movements between these locations, such as A* [5], Dijkstra's algorithm [4], D* [6], and JPS (Jump Point Search) [7]. The second approach comprises sampling-based techniques, including Probabilistic Roadmaps (PRM) [8] and rapidly exploring random trees (RRTs) [9]. These algorithms randomize the search space into samples and construct paths based on these samples. The third approach involves Artificial Potential Fields [10], where attractive forces guide the UAV (Unmanned Aerial Vehicle) toward the goal. Recently, bio-inspired algorithms have been utilized to address path-planning challenges. These algorithms draw inspiration from biological phenomena like animal behavior and rely on a predefined cost function. Examples include ant colony optimization (ACO) [11], particle swarm optimization (PSO) [12], and grey wolf optimization (GWO) [13]. Each of these methods has its advantages. However, there are still many challenges associated with using these approaches, and no single algorithm is suitable for all scenarios. For example, graph-based methods are computationally expensive, especially in 3D spaces and large environments [14]. Bio-inspired methods require parameter tuning and may necessitate running simulations for numerous generations to find a good solution [15]. APF (Artificial Potential Field) methods can be easily trapped in local minima, particularly when navigating close to obstacles [16]. Sampling-based methods typically provide a series of waypoints rather than a smooth, continuous trajectory, which can be challenging for UAVs with complex dynamics that require precise motion control [17]. Among these algorithms, RRT* [18], A*, and PSO are classical methods frequently employed in various path-planning scenarios. This paper specifically addresses the UAV path planning challenge within an urban 3D environment. It compares and analyzes the advantages of the three classical algorithms under different flying conditions. To effectively choose the best path planning algorithm, six different scenarios are designed and applied, considering environment size, various obstacle sizes, densities, and shapes, as well as different altitudes between the start and the target positions.

The structure of the paper is as follows: Section 2 reviews related comparison studies in the field. Section 3 presents a concise summary of the three most commonly used algorithms: A*, RRT*, and PSO. Section 5 details the simulation and Analysis. Section 6 presents the conclusion.

II. RELATED WORKS

Several studies have compared these algorithms in the field of path planning. For instance, Zakir et al. [19] evaluate an improved Dijkstra algorithm combined with a Voronoi diagram and the A* algorithm to minimize threat collisions and fuel consumption. The results found that the Voronoi-Dijkstra approach is effective in stable environments, while A* finds paths between nodes using an effective heuristic. Kevin et al. [20] compare Dijkstra's and waypoint generation algorithms. The study evaluates both algorithms across various scenarios, and the results show that Dijkstra offers precise solutions, but its performance varies depending on the cost function. However, The heuristic waypoint generation method provides a simple and faster search but sometimes has collision. Zammit et al. [21] evaluate A* and RRT algorithms for 3D UAV path planning in complex scenarios with vertical and horizontal obstacles. Their study shows that A* consistently offers shorter path lengths and faster generation times than RRT, making it the more efficient choice for online 3D navigation. Ziang et al. [22] compare three path planning algorithms: A*, RRT, and ACO for UAV path planning in complex 3D city environments. The study finds that A* performs consistently well, ACO is best for large-scale scenarios with significant height differences, and RRT generally fails due to its randomness technique. Hu et al. [23] compare Genetic Algorithms (GA), Ant Colony Optimization (ACO), and Particle Swarm Optimization (PSO) for optimizing mission performance for UAVs. The experimental findings show that GA is better in complex environments, ACO is effective for multiple nodes, and PSO is best for real-time tasks.

III. THE THREE UTILIZED ALGORITHMS DESCRIPTION

In this section, the paper briefly explains the algorithms, namely A*, RRT*, and PSO.

A. A* Algorithm

A* is a graph-based algorithm that finds a path between two nodes in grids or graphs. It is a variant of the Dijkstra algorithm but uses a heuristic function to guide the search and ensure the minimization of the path length. A* usually solves path-finding problems and is often used in UAV missions [24]. To effectively explore the entire nodes, A* uses two sets: an open set and a closed set. The open set is used to store unexplored nodes, and the closed set is used for the explored ones. The heuristic function is used to calculate and define the chosen path and ensures the choice of the best one. The function is defined as follows:

$$f(n) = g(n) + h(n) \quad (1)$$

Algorithm 1 A* Algorithm

```

1: Input: start as the Start node ,and goal as The Goal node
2: Output: Final Path
3: Initialize the openlist with start
4: Initialize  $g(start)$  to 0
5: Set  $f(start) = g(start) + h(start)$ 
6: while openlist is not empty do
7: State Set Current to the node in the open list with the
   smallest  $f$  value
8:   if Current reached the goal node then
9:     return the path by reconstructing it from the goal node
10:  end if
11:  Move the current node Current from openlist to
   closedlist
12:  for each neighbor of Current do
13:     $g\_score \leftarrow g(Current) + cost(Current, neighbor)$ 
14:    if neighbor is in closedlist and  $g\_score \geq$ 
    $g(neighbor)$  then
15:      continue
16:    end if
17:    if neighbor is not in openlist or  $g\_score <$ 
    $g(neighbor)$  then
18:      Set parent of neighbor to Current
19:      Set  $g(neighbor) = g\_score$ 
20:      Set  $f(neighbor) = g(neighbor) + h(neighbor)$ 
21:      if openlist do not contains neighbor then
22:        Store neighbor in the openlist
23:      end if
24:    end if
25:  end for
26: end while
27: return failure

```

Fig. 1: A* algorithm pseudo-code

The equation uses $g(n)$ for the actual cost from the start to node n and $h(n)$ for the estimated cost to the goal. The heuristic $h(n)$ must be admissible, and the true cost must never be overestimated.

To effectively plan a path in a specific environment, the algorithm first initializes two empty lists: an *openlist* and a *closedlist*. The starting node is then added to the *openlist*. For each node, the algorithm calculates its f value using Equation 1. Next, the algorithm repeatedly selects the node with the lowest f value from the *openlist*. It checks if this node is the goal; if so, the path is found and reconstructed from the goal to the start. Otherwise, the node is moved to the *closedlist*, and its neighbors are evaluated. This process continues until the goal is reached or the *openlist* becomes empty.

The A* algorithm's pseudo code is outlined in Fig.1

Despite the simplicity of the A* algorithm, it has disadvantages. Firstly, the algorithm struggles in high-dimensional spaces and can be computationally expensive in execution time and storage due to the open and closed lists. In UAV path planning, the algorithm cannot guarantee the optimal path due to the limited number of each node's neighbors and the heuristic function [24].

Algorithm 2 RRT* Algorithm

```
1: Inputs: Initial state  $x_{init}$ , the number of iterations  $It$ 
2: Output: The Final RRT* tree  $T$ 
3: Initialization of the tree  $T$  with the root node  $x_{init}$ 
4: for  $k = 1$  to  $K$  do
5:   Generate  $x_{rand}$  which is a random state
6:   Determine  $x_{nearest} \in T$  (nearest node) to  $x_{rand}$ 
7:    $x_{new} \leftarrow \text{Steer}(x_{nearest}, x_{rand})$   $\triangleright$  Steer function to
   generate a new node
8:   if Obstacle-free( $x_{nearest}, x_{new}$ ) then
9:
10:    Locate the set of nearby nodes  $N_{near} \subseteq T$ 
11:    Choose the parent  $x_{min}$  from  $N_{near}$  that minimizes
     $J(x_{min}) + c(x_{min}, x_{new})$ 
12:    Add  $x_{new}$  to  $T$  with parent  $x_{min}$ 
13:    for all  $x_{near} \in N_{near}$  do
14:      if  $J(x_{new}) + c(x_{new}, x_{near}) < J(x_{near})$  then
15:        Update parent of  $x_{near}$  to  $x_{new}$ 
16:      end if
17:    end for
18:  end if
19: end for
20: return  $T$ 
```

Fig. 2: RRT* algorithm pseudo-code

B. RRT* Algorithm

RRT* is a variation and an enhanced version of the Rapidly-exploring Random Tree (RRT) algorithm, designed to efficiently find optimal paths in high-dimensional spaces. The RRT algorithm is sampling-based, utilizing the search space to construct a random tree structure that begins from an initial position. It iteratively expands this tree by connecting each sampled point to the nearest node in the tree.

Unlike RRT, which focuses on rapidly exploring the space and identifying any feasible path between the start and the target points, RRT* aims to discover the optimal path. Its basic idea is to use the existing tree and dynamically rewire it to improve path quality over time. The algorithm starts with the starting point position. In each step, it randomly selects a new position in the search space to explore. It then finds the closest one in the path tree to this new position. The algorithm checks if this subpath collides with obstacles. If not, the newly created point is added to the tree, and the connection is returned to the closest existing node. Unlike basic RRT, RRT* also checks nearby nodes to see if they can find better routes through the new node. This process continually refines the tree structure to find the best possible path through the space [25]. The RRT* algorithm pseudo code is in Fig.2

RRT* is a popular algorithm for UAV path planning due to its effectiveness in navigating complex and high-dimensional environments. However, it has several limitations. The solution it finds is often only near-optimal due to the randomized sampling. Another limitation is that RRT* can find difficulty in

finding feasible paths in environments with narrow channels. That means it depends on luck instead of calculations to find a path in these small areas [26].

C. Particle Swarm Optimization (PSO)

PSO is a bio-inspired algorithm created in 1995 by J. Kennedy and R. Eberhart [12]. The algorithm utilizes a bio-inspired approach based on bird and fish foraging. PSO is widely used in path planning applications and can find the optimal route in different environments [27]. In PSO, the particles, which are a population of candidate solutions, navigate the search space to find the best or near-best solution. In each iteration, the particles update their positions based on two key factors: their own personal best positions ($pbest$) and the global best position ($gbest$) found within the entire population. This process continues iteratively until a specified number of iterations is reached. The quality of the solution is determined by a fitness function that evaluates each particle's position. This function, also known as the objective function, gives each particle a value, which represents its performance relative to the optimization goal. The fitness function is essential for guiding the swarm towards better solutions in the space. The equations used to adjust each particle's position and velocity are as follows:

$$v_{i,d}^{t+1} = \omega v_{i,d}^t + c_1 r_1 (pbest_{i,d}^t - x_{i,d}^t) + c_2 r_2 (gbest_d^t - x_{i,d}^t) \quad (2)$$

$$x_{i,d}^{t+1} = x_{i,d}^t + v_{i,d}^{t+1} \quad (3)$$

Where $v_{i,d}^t$ and $v_{i,d}^{t+1}$ denote the i -th particle velocity at iteration t and $t+1$ within d dimension respectively, ω represents the inertia weight. $pbest_{i,d}^t$ in the previous equation is the personal best position and $gbest_d^t$ is the global best position of the i -th particle at iteration t and dimension d . c_1 and c_2 are both learning factors. To be specific, c_1 is the self-learning factor that determines how much a particle relies on its individual experience when determining its future movements. Higher values of c_1 mean that particles are increasingly influenced by their ($pbest$). c_2 is the social learning factor, also referred to as the social acceleration factor, which represents a particle's tendency to move toward the best solutions discovered by any member of the swarm. Its primary function is to draw the particle toward the ($gbest$). r_1 and r_2 are a random numbers varying between 0 and 1, $x_{i,d}^t$ represents the i -th particle's current position, d is for dimension and t for iteration number. The RRT* algorithm pseudo code is in Fig.3

Bio-inspired algorithms such as PSO are widely used in UAV path planning applications to find the shortest path from the start to the target point. However, these techniques may suffer from several limitations. Firstly, when planning a path in high-dimensional space, particles require significant computational resources and a large number of iterations. Secondly, due to the random movement of PSO particles, there is a risk of failing to find optimal solutions. Thirdly, The effectiveness of PSO is significantly influenced by its

Algorithm 3 Particle Swarm Optimization (PSO)

```
1: Inputs:  $\omega$ ,  $c_1$ ,  $c_2$ , Number of particles  $N$ , Maximum iterations  $T$ 
2: Output: The Global best position  $gbest$ 
3: Initialize particle positions  $\{x_{i,d}^0\}$  and velocities  $\{v_{i,d}^0\}$  for  $i = 1, \dots, N$  and  $d = 1, \dots, D$ 
4: Initialize each particle's personal best  $pbest_{i,d}^0 = x_{i,d}^0$  for  $i = 1, \dots, N$  and  $d = 1, \dots, D$ 
5: Initialize  $gbest$  as the best position among all  $pbest$ 
6: for  $t = 0$  to  $T$  do
7:   for  $i = 1$  to  $N$  do
8:     for  $d = 1$  to  $D$  do
9:       Generate random numbers  $r_1$  and  $r_2$  uniformly in  $[0, 1]$ 
10:      Update the velocity according to Equation 2.
11:      Update the position according to Equation 3
12:    end for
13:    if  $f(x_i^{t+1}) < f(pbest_i^t)$  then
14:       $pbest_{i,d}^{t+1} = x_{i,d}^{t+1}$ 
15:    end if
16:  end for
17:  if any  $f(pbest_i^{t+1}) < f(gbest^t)$  then
18:     $gbest_d^{t+1} = pbest_{i,d}^{t+1}$  for the best  $i$ 
19:  end if
20: end for
21: return  $gbest$ 
```

Fig. 3: PSO algorithm pseudo-code

highly sensitive parameters. These selected parameters include population size, inertia weight, and both cognitive and social coefficients. Finding the right combination of parameters is challenging and requires multiple experiments [28].

IV. SIMULATIONS AND ANALYSIS

The following experiment and algorithm were conducted on a MacBook Pro 2020 with an i5 processor and 8GB RAM, running MATLAB 2023a.

A. Environment Modelling

In a real-world 3D environment, UAVs encounter various challenges. For instance, they must sometimes avoid a single obstacle and, at other times, multiple obstacles simultaneously. Additionally, UAVs may need to operate at varying altitudes, either high or low. To evaluate the effectiveness of the three algorithms and make a comparative analysis, this paper employs 3 distinct experiments with two different scenarios each.

1) *Experiment 1: Obstacle Density Variation:* The first scenario sets obstacles at a high density of 60%, which creates a densely urban environment intended to challenge pathfinding algorithms with numerous obstacles. Conversely, the second scenario reduces obstacle density to 10%. This results in a less challenging environment with more open spaces and fewer obstacles. These scenarios aim to evaluate algorithm performance across different urban conditions and highlight their adaptability and efficiency in navigating varying levels of spatial complexity.

2) *Experiment 2: Travel Distance Variation:* This experiment investigates how three algorithms perform under varying travel distances across maps of different sizes. In Scenario 3, the algorithms are tested over a long travel distance between the start and endpoint on a large city map of 2 km by 2 km. This scenario evaluates their efficiency, reliability, and ability to maintain optimal pathfinding strategies over extended distances. Conversely, Scenario 4 tests the algorithms over a short travel distance on a smaller map of 1 km by 1 km, which challenges the three algorithms with shorter navigation tasks.

3) *Experiment 3: Altitude Variation:* This experiment evaluates three algorithms' performance in navigating urban environments with different altitude conditions. Scenario 5 tests the algorithms with significant altitude differences between the start and endpoint. This challenges their pathfinding abilities over diverse urban terrains. Meanwhile, Scenario 6 examines their navigation capabilities when the start and endpoint are at the same altitude level within the city.

In addition, several constraints must be considered when testing three algorithms for path-planning missions. Firstly, to ensure safe collision avoidance, this paper sets a security distance of 1 m between the generated path and obstacles. Moreover, in Experiment 3, the algorithms are tested at different altitudes, with a maximum altitude difference of 30 m between the start and target points. Additionally, this paper considers battery life constraints by using a limited flying range of 200 m for all scenarios except Scenario 4 (2 km x 2 km), where the maximum range is 400 m. Furthermore, any sharp turns less than 30 degrees are considered unsuitable for the planned path and will not be considered. This paper uses the Euclidean distance for the A* algorithm's heuristic function. For the RRT* algorithm, the random choosing rate is set to 0.5. For the PSO algorithm, the paper selects 200 for the iteration number, 150 for the population size, and 1.9 for both c_1 and c_2 learning factors.

B. Evaluation Metrics

To effectively test the three algorithms' efficacy and performance, three objective functions have been adopted, including path distance, number of turning angles, and algorithm running time.

1) *Path Length P :* While path length directly reduces travel time, choosing the shortest path is essential for the path planning algorithm's objective function. The following function is used to calculate the path length P :

$$L = \sum_{i=1}^{n-1} \sqrt{(x_{i+1} - x_i)^2 + (y_{i+1} - y_i)^2 + (z_{i+1} - z_i)^2} \quad (4)$$

where n denotes the number of nodes, x_i , y_i , and z_i are the coordinates of each node i in the path.

2) *Number Of Turning Angles:* The number of turning angles significantly impacts UAV path efficiency, stability, and maneuverability. Each turn affects path length, flight stability,

and the UAV's ability to navigate obstacles and execute mission objectives effectively. The following formula is used:

$$T_r(\theta) = \sum_{i=1}^{n-1} \theta_i. \quad (5)$$

$$\vec{a} = (x_n - x_{n-1}, y_n - y_{n-1}, z_n - z_{n-1}) \quad (6)$$

$$\vec{b} = (x_{n+1} - x_n, y_{n+1} - y_n, z_{n+1} - z_n) \quad (7)$$

$$\cos \theta_n = \frac{\vec{a} \cdot \vec{b}}{\|\vec{a}\| \|\vec{b}\|} \quad (8)$$

Here, n represents the n -th path node, and θ_n is the angle at the n -th node, calculated based on the positions of the nodes $n-1$, n , and $n+1$. \vec{a} and \vec{b} are two vectors calculated based on the $n-1$, n , and $n+1$ path nodes. $|\vec{a}|$ and $|\vec{b}|$ are the magnitudes of \vec{a} and \vec{b} , respectively.

3) *Algorithm Time*: the execution time of the algorithm strongly influences the overall mission operation time. Therefore, an objective function is defined as follows:

$$T_{alg} = toc - tic \quad (9)$$

Where toc and tic are predefined instructions to calculate the time of the algorithm using Matlab Toolbox

C. Experiment Analysis And Comparison

As shown in Fig.4a, The A* algorithm always chooses the lowest cost path, which makes the UAV fly close to obstacles and at low altitudes. However, this path has many turns, making UAVs consume more energy. Conversely, the planned path using the RRT* algorithm, shown in Fig.4b, has even more turns due to its random sampling strategy. Some of these turns are sharp, adversely affecting the UAV's dynamics. Finally, as seen in Fig.4c, the path generated by the PSO algorithm forms approximately a straight line connecting the start and the goal points. This planned trajectory allows the UAV to make small angle adjustments, resulting in lower energy consumption.

As shown in Fig. 5, three paths generated by A*, RRT*, and PSO algorithms are compared under different conditions. Fig. 5a and Fig. 5b represent Experiment 1, which tests path planning under varying obstacle densities. We observe that the paths planned by the three algorithms in Fig. 5a are shorter, have fewer turning points, and maintain a lower altitude range compared to the paths generated in Fig. 5b. Experiment 2, represented by Fig.5c and Fig.5d, test the algorithms under different altitudes. It demonstrates that the A* algorithm and PSO produce nearly straight lines, while RRT* continues to generate random nodes at lower altitudes. Unlike Experiment 1, The A* uses the absence of obstacles at a high altitude to minimize the turns. Fig.5e shows the results of Experiment 3, which is described in the previous section. From the results in Fig.5e, it is obvious that generated paths are longer compared to Fig.5f because of the size of the map.

Fig.6 shows the comparison of path length (km), the sum of turning angles (rad), and the algorithm time (s) under the

same scenarios. From Fig.6a, we can see that the A* algorithm consistently produces the shortest paths, outperforming RRT* and PSO. On average, the path length for A* is about 20% shorter than RRT* and around 5% shorter than PSO. Additionally, both the map's size and the density of obstacles significantly impact the path length.

When examining the sum of turning angles in Fig.6b, particularly in handling tight turns. On average, PSO's turning radius is approximately 85% smaller than that of RRT* and about 70% smaller than that of A*. For example, in map scenario 'f,' PSO achieves a turning radius of 3 rad, which is 90% smaller than RRT*'s turning radius of 30.13 rad and approximately 67% smaller than A*'s turning radius of 9.25 rad. This significant reduction in turning radius indicates that PSO is more adept at navigating through tighter spaces than RRT* and A*.

Regarding computation times, A* is the most efficient algorithm, often completing its calculations in a fraction of the time taken by RRT* and PSO. A* is typically 90% faster than PSO and about 75% faster than RRT*. For instance, in map scenario 'e', A* completes in 4.6759 seconds, which is approximately 76% faster than RRT*'s 19.7987 seconds and a remarkable 97% faster than PSO's 141.3934 seconds.

V. CONCLUSION

From the findings discussed above, it is evident that the A* is the preferred algorithm for UAV path planning due to its optimal path length and rapid computation time, making it highly effective for navigation. PSO's ability to handle tight turns and dense environments makes it a valuable algorithm in specific scenarios, but its high computation time is a drawback. RRT* offers a balance but falls short in comparison to A*'s overall efficiency due to its randomness.

VI. DECLARATION OF INTERSETS

The authors report no conflicts of interest relevant to this study.

VII. DATA AVAILABILITY

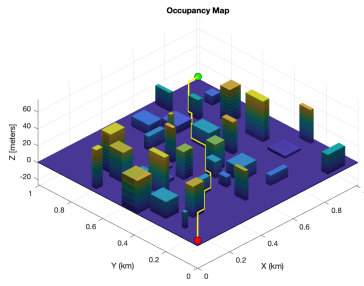
Data can be obtained upon request.

ACKNOWLEDGMENT

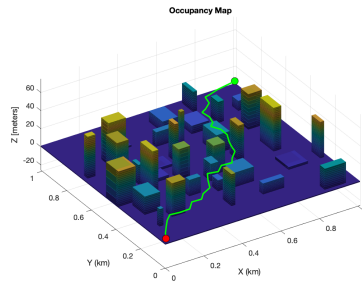
This work was supported by the research project "Modeling and Control of Aerial Manipulators" N° C00L07UN310220230004.

REFERENCES

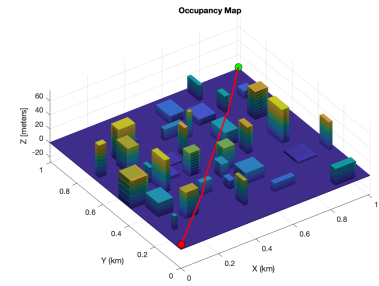
- [1] Huang, X., Dong, X., Ma, J., Liu, K., Ahmed, S., Lin, J., & Qiu, B. (2021). The Improved A* Obstacle Avoidance Algorithm for the Plant Protection UAV with Millimeter Wave Radar and Monocular Camera Data Fusion. *Remote Sensing* 2021, Vol. 13, Page 3364, 13(17), 3364. <https://doi.org/10.3390/RS13173364>
- [2] C. Wu, X. Huang, Y. Luo and S. Leng, "An Improved Fast Convergent Artificial Bee Colony Algorithm for Unmanned Aerial Vehicle Path Planning in Battlefield Environment," 2020 IEEE 16th International Conference on Control & Automation (ICCA), Singapore, 2020, pp. 360-365, doi: 10.1109/ICCA51439.2020.9264555.
- [3] Póika, M., Ptak, S., & Kuziora, Ł. (2017). The Use of UAV's for Search and Rescue Operations. *Procedia Engineering*, 192, 748-752. <https://doi.org/10.1016/J.PROENG.2017.06.129>



(a) A* Algorithm

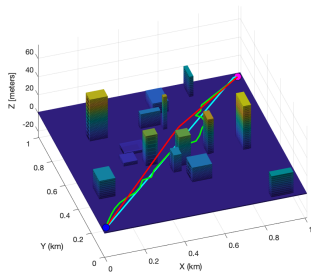


(b) RRT* Algorithm

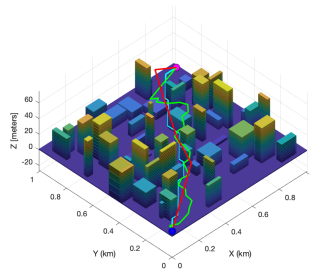


(c) PSO Algorithm

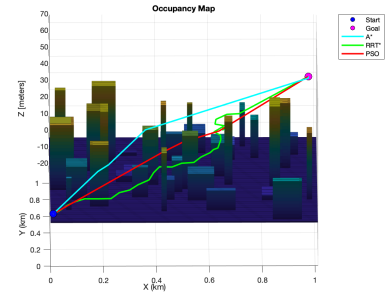
Fig. 4: Generated Paths Using A*, RRT* and PSO Algorithms



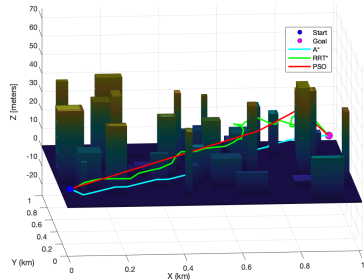
(a) Less Obstacles



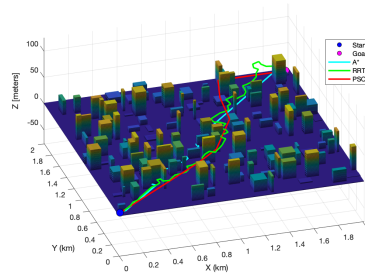
(b) Dense Obstacles



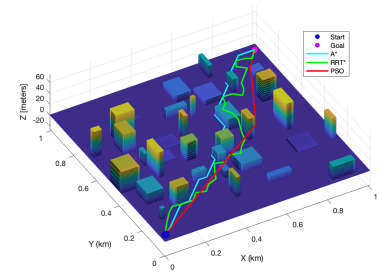
(c) Large Altitude Difference



(d) Short Altitude Difference

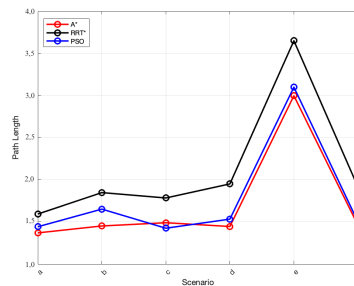


(e) Large Map

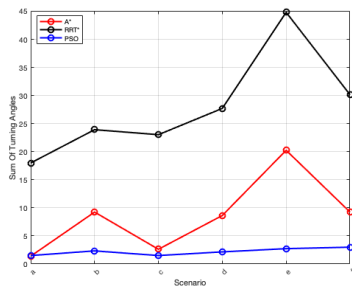


(f) Small Map

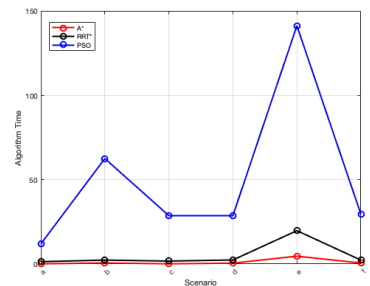
Fig. 5: Comparisons of Generated Paths Under Different Scenarios



(a) Path Length



(b) Turning Angles



(c) Algorithm Time

Fig. 6: Comparison of various metrics (a) Path Length, (b) Turning Radius, and (c) Algorithm Computation Time across different algorithms and map scenarios.

- [4] Dijkstra, E. W. (1959). A note on two problems in connexion with graphs. *Numerische Mathematik*, 1(1), 269–271. <https://doi.org/10.1007/BF01386390/METRICES>
- [5] Hart, P. E., Nilsson, N. J., & Raphael, B. (1968). A Formal Basis for the Heuristic Determination of Minimum Cost Paths. *IEEE Transactions on Systems Science and Cybernetics*, 4(2), 100–107. <https://doi.org/10.1109/TSSC.1968.300136>
- [6] Stentz, A. (n.d.). Optimal and efficient path planning for partially-known environments. *Proceedings of the 1994 IEEE International Conference on Robotics and Automation*, 3310–3317. <https://doi.org/10.1109/ROBOT.1994.351061>
- [7] Harabor, D., & Grastien, A. (2011). Online Graph Pruning for Pathfinding on Grid Maps. *Proceedings of the AAAI Conference on Artificial Intelligence*, 25(1), 1114–1119. <https://doi.org/10.1609/AAAI.V25I1.7994>
- [8] Kavraki, L. E., Švestka, P., Latombe, J. C., & Overmars, M. H. (1996). Probabilistic roadmaps for path planning in high-dimensional configuration spaces. *IEEE Transactions on Robotics and Automation*, 12(4), 566–580. <https://doi.org/10.1109/70.508439>
- [9] LaValle, S. (1998). Rapidly-Exploring Random Trees: A New Tool for Path Planning.
- [10] Park, M. G., & Lee, M. C. (2003). Artificial potential field based path planning for mobile robots using a virtual obstacle concept. *IEEE/ASME International Conference on Advanced Intelligent Mechatronics, AIM*, 2, 735–740. <https://doi.org/10.1109/AIM.2003.1225434>
- [11] Dorigo, M., & di Caro, G. (1999). Ant colony optimization: A new meta-heuristic. *Proceedings of the 1999 Congress on Evolutionary Computation, CEC 1999*, 2, 1470–1477. <https://doi.org/10.1109/CEC.1999.782657>
- [12] Kennedy, J., & Eberhart, R. (n.d.). Particle swarm optimization. *Proceedings of ICNN'95 - International Conference on Neural Networks*, 4, 1942–1948. <https://doi.org/10.1109/ICNN.1995.488968>
- [13] Mirjalili, S., Mirjalili, S. M., & Lewis, A. (2014). Grey Wolf Optimizer. *Advances in Engineering Software*, 69, 46–61. <https://doi.org/10.1016/j.ADVENGSOFT.2013.12.007>
- [14] Yang, F., Lee, D.-H., Keller, J., & Scherer, S. (n.d.). Graph-based Topological Exploration Planning in Large-scale 3D Environments.
- [15] Darwish, A. (2018). Bio-inspired computing: Algorithms review, deep analysis, and the scope of applications. *Future Computing and Informatics Journal*, 3(2), 231–246. <https://doi.org/10.1016/j.FCIJ.2018.06.001>
- [16] Park, M. G., & Lee, M. C. (2003). A new technique to escape local minimum in artificial potential field based path planning. *KSMIE International Journal* 2003 17:12, 17(12), 1876–1885. <https://doi.org/10.1007/BF02982426>
- [17] Lindemann, S. R., & LaValle, S. M. (2005). Current Issues in Sampling-Based Motion Planning. *Springer Tracts in Advanced Robotics*, 15, 36–54. <https://doi.org/10.1007/110089415>
- [18] Karaman, S., & Frazzoli, E. (2011). Sampling-based Algorithms for Optimal Motion Planning. *ArXiv. /abs/1105.1186*
- [19] Zakir, R. (n.d.). Comparative Study of UAV Path Planning Algorithms. *Middle East Journal of Applied Science & Technology (MEJAST) (Peer Reviewed & Quarterly International Journal*, 2(2), 17–20.
- [20] Danancier, K., Ruvio, D., Sung, I., & Nielsen, P. (2019). Comparison of Path Planning Algorithms for an Unmanned Aerial Vehicle Deployment Under Threats. *IFAC-PapersOnLine*, 52(13), 1978–1983. <https://doi.org/10.1016/j.IFACOL.2019.11.493>
- [21] Zammit, C., & van Kampen, E. J. (2022). Comparison Between A* and RRT Algorithms for 3D UAV Path Planning. *Unmanned Systems*, 10(2), 129–146. <https://doi.org/10.1142/S2301385022500078>
- [22] Gao, Z., Zhang, X., Li, Y., Zhu, Y., Wu, H., & Guan, X. (2022). Analyses and Comparisons of UAV Path Planning Algorithms in Three-Dimensional City Environment. *IEEE Conference on Intelligent Transportation Systems, Proceedings, ITSC*, 2022-October, 459–464. <https://doi.org/10.1109/ITSC55140.2022.9922063>
- [23] Hu, D., Kuang, Y., & Zhang, T. (2023). Comparative Analysis of Algorithms and Applications in Unmanned Aerial Vehicle Path Planning in Recent Years. *Advances in Computer Science Research*, 108, 431–446. https://doi.org/10.2991/978-94-6463-300-9_44
- [24] Aggarwal, S., & Kumar, N. (2020). Path planning techniques for unmanned aerial vehicles: A review, solutions, and challenges. *Computer Communications*, 149, 270–299. <https://doi.org/10.1016/j.COMCOM.2019.10.014>
- [25] Noreen, I., Khan, A., & Habib, Z. (2016). A Comparison of RRT, RRT* and RRT*-Smart Path Planning Algorithms.
- [26] Guo, J., Xia, W., Hu, X., & Ma, H. (2022). Feedback RRT* algorithm for UAV path planning in a hostile environment. *Computers & Industrial Engineering*, 174, 108771. <https://doi.org/10.1016/J.CIE.2022.108771>
- [27] Agrawal, S., Patle, B. K., & Sanap, S. (2024). A systematic review on metaheuristic approaches for autonomous path planning of unmanned aerial vehicles. *Drone Systems and Applications*, 12, 1–28. <https://doi.org/10.1139/DSA-2023-0093>
- [28] Aljaleud, F., Kurdi, H., & Youcef-Toumi, K. (2023). Bio-Inspired Multi-UAV Path Planning Heuristics: A Review. *Mathematics* 2023, Vol. 11, Page 2356, 11(10), 2356. <https://doi.org/10.3390/MATH11102356>
- [29] Price, K. v. (2013). *Differential Evolution. Intelligent Systems Reference Library*, 38, 187–214. https://doi.org/10.1007/978-3-642-30504-7_8
- [30] da Silva, I. N., Spatti, D. H., Flauzino, R. A., Liboni, L. H. B., & dos Reis Alves, S. F. (2016). Artificial neural networks: A practical course. *Artificial Neural Networks: A Practical Course*, 1–307. <https://doi.org/10.1007/978-3-319-43162-8/COVER>
- [31] Cortes, C., Vapnik, V., & Saïtta, L. (1995). Support-vector networks. *Machine Learning* 1995 20(3), 273–297. <https://doi.org/10.1007/BF00994018>
- [32] Besseded, A., Gargaro, M., Pallotta, M. T., Matino, D., Servillo, G., Brunacci, C., Bacciato, S., Mazza, E. M. C., Macchiarulo, A., Vacca, C., Iannitti, R., Tissi, L., Volpi, C., Belladonna, M. L., Orabona, C., Bianchi, R., Lanz, T. v., Platten, M., della Fazio, M. A., ... Puccetti, P. (2017). Deep Reinforcement Learning: An Overview. *ArXiv.Org*, 511(7508), 184–190. <http://arxiv.org/abs/1810.06339>
- [33] Roberge, V., Tarbouchi, M., & Allaire, F. (2014). Parallel hybrid meta-heuristic on shared memory system for real-time UAV path planning. *International Journal of Computational Intelligence and Applications*, 13(2). <https://doi.org/10.1142/S1469026814500084>
- [34] Yang, K., Keat Gan, S., & Sukkarieh, S. (2013). A Gaussian process-based RRT planner for the exploration of an unknown and cluttered environment with a UAV. *Advanced Robotics*, 27(6), 431–443. <https://doi.org/10.1080/01691864.2013.756386>
- [35] Maini, P., & Sujit, P. B. (2016). Path planning for a UAV with kinematic constraints in the presence of polygonal obstacles. *International Conference on Unmanned Aircraft Systems*, 62–67. <https://doi.org/10.1109/ICUAS.2016.7502625>
- [36] Lee, D., & Shim, D. H. (2016). Path planner based on bidirectional spline-RRT* for fixed-wing UAVs. *2016 International Conference on Unmanned Aircraft Systems, ICUAS 2016*, 77–86. <https://doi.org/10.1109/ICUAS.2016.7502539>
- [37] Karaman, S., & Frazzoli, E. (2011). Sampling-based algorithms for optimal motion planning. *International Journal of Robotics Research*, 30(7), 846–894. <https://doi.org/10.1177/0278364911406761>
- [38] Wu, X., Xu, L., Zhen, R., & Wu, X. (2020). Bi-Directional Adaptive A* Algorithm Toward Optimal Path Planning for Large-Scale UAV under Multi-Constraints. *IEEE Access*, 8, 85431–85440. <https://doi.org/10.1109/ACCESS.2020.2990153>
- [39] Zhang, Z., Wu, J., Dai, J., & He, C. (2022). Optimal path planning with modified A-Star algorithm for stealth unmanned aerial vehicles in 3D network radar environment. *Proceedings of the Institution of Mechanical Engineers, Part G: Journal of Aerospace Engineering*, 236(1), 72–81. <https://doi.org/10.1177/09544100211007381>
- [40] Bashir, N., Boudjit, S., Dauphin, G., & Zeadally, S. (2023). An obstacle avoidance approach for UAV path planning. *Simulation Modelling Practice and Theory*, 129, 102815. <https://doi.org/10.1016/J.SIMPAT.2023.102815>
- [41] Liu, H., Li, X., Fan, M., Wu, G., Pedrycz, W., & Nagarathnam Suganthan, P. (2022). An Autonomous Path Planning Method for Unmanned Aerial Vehicle Based on a Tangent Intersection and Target Guidance Strategy. *IEEE Transactions on Intelligent Transportation Systems*, 23(4), 3061–3073. <https://doi.org/10.1109/TITS.2020.3030444>
- [42] Luo, W., Chen, J., Ebel, H., & Eberhard, P. (2022). Time-Optimal Handover Trajectory Planning for Aerial Manipulators based on Discrete Mechanics and Complementarity Constraints. <http://arxiv.org/abs/2209.00533>
- [43] Liu, H., Wu, G., Zhou, L., Pedrycz, W., & Suganthan, P. N. (2023). Tangent-Based Path Planning for UAV in a 3-D Low Altitude Urban Environment. *IEEE Transactions on Intelligent Transportation Systems*, 24(11), 12062–12077. <https://doi.org/10.1109/TITS.2023.3285568>
- [44] Zafar, M. M., Anjum, M. L., & Hussain, W. (2021). LTA*: Local tangent based A* for optimal path planning. *Autonomous Robots*, 45(2), 209–227. <https://doi.org/10.1007/S10514-020-09956-3/METRICES>

- [45] Liu, M., Zhang, H., Yang, J., Zhang, T., Zhang, C., & Bo, L. (2024). A path planning algorithm for three-dimensional collision avoidance based on potential field and B-spline boundary curve. *Aerospace Science and Technology*, 144, 108763. <https://doi.org/10.1016/J.AST.2023.108763>
- [46] Li, Y., Zhang, L., Cai, B., & Liang, Y. (2024). Unified path planning for composite UAVs via Fermat point-based grouping particle swarm optimization. *Aerospace Science and Technology*, 148, 109088. <https://doi.org/10.1016/J.AST.2024.109088>
- [47] Liu, Y. H., & Arimoto, S. (1992). Path Planning Using a Tangent Graph for Mobile Robots Among Polygonal and Curved Obstacles. *The International Journal of Robotics Research*, 11(4), 376–382. <https://doi.org/10.1177/027836499201100409>
- [48] Switching, E. M.-I. S. on the T. of, & 1959, undefined. (n.d.). The shortest path through a maze. *Cir.Nii.Ac.Jp*. Retrieved June 10, 2024, from <https://cir.nii.ac.jp/crid/1570572700914359680>